

Characterization of thermo-sensitive hydrogels based on poly(*N*-isopropylacrylamide)/hyaluronic acid

Ramón Coronado · Sara Pekerar ·
Arnaldo T. Lorenzo · Marcos A. Sabino

Received: 15 July 2010/Revised: 1 November 2010/Accepted: 6 November 2010/
Published online: 16 November 2010
© Springer-Verlag 2010

Abstract In this study, an hydrogel was synthesized from the monomer *N*-isopropylacrylamide (NIPA), generating the poly(*N*-isopropylacrylamide) (PNIPA) and other formulations were synthesized in the presence of 1, 2, and 3% hyaluronic acid (HA) for obtain an interpenetrating polymer network. For all the obtained hydrogels, the thermo-sensitive response was studied since the lower critical solution temperature (LCST) and was analyzed by differential scanning calorimetry (DSC), nuclear magnetic resonance (NMR), and oscillatory rheology at constant frequency as a function of temperature. The LCST transition temperature ($T_{t\ onset}$) was found between 34.4 and 35.5 °C. By scanning electron microscopy (SEM) PNIPA-HA formulations showed a porous morphology. The applicability of the hydrogels as injectable and non-toxic materials was verified, respectively, by rheology results and by cytotoxicity studies through an in vitro test of cell hemolysis on blood agar.

Keywords Poly-NIPA · Hyaluronic acid · Thermo-sensitive · Interpenetrating polymer network · Injectable hydrogel

R. Coronado · M. A. Sabino (✉)
B5IDA Group, Department of Chemistry, Universidad Simón Bolívar,
Apartado 89000, Caracas 1080, Venezuela
e-mail: msabino@usb.ve

S. Pekerar
IVIC, Venezuelan Institute of Scientific Research, Chemistry Center,
Altos de Pipe, Estado Miranda, Venezuela

A. T. Lorenzo
USB Polymer Group, Department of Materials Science, Universidad Simón Bolívar,
Apdo. 89000, Caracas 1080, Venezuela

Introduction

Hydrogels are defined as hydrophilic polymers which, due to their structural network, can absorb water without being soluble under physiological conditions of temperature, pH, and ionic strength. Crosslinks can be formed by covalent, electrostatic, or hydrophobic bonds, or dipole–dipole interactions [1]. Hydrogels may be classified as synthetic, natural, smart, and biodegradable; and depending on their preparation method, hydrogels are classified as crosslinked by free-radical polymerization, crosslinked by irradiation, and crosslinked by physical interactions [1–3].

Finally, they are known as smart or conventional hydrogels depending on the capability they have to show significant dimensional changes as a response to applied stimuli or changes in pH, temperature, electric field, etc. [4], and they deserve to be in a class of their own. What is most interesting is that these changes are reversible once the stimulus is removed [3, 4]. In the case of thermally sensitive smart polymers in solution, the stimuli-induced changes are related to a lower critical solution temperature or LCST, a specific temperature at which the polymer solution shows phase separation to result in a polymer-rich phase and a solvent-rich phase [5, 6]. In hydrogels, which are crosslinked structures, the LCST system describes the thermodynamic equilibrium for the polymer chains between cross-linking points, which are insoluble and infusible.

Poly(*N*-isopropylacrylamide) PNIPA (Fig. 1a) is non-biodegradable polymer which has a LCST phase transition at about 32 °C when dissolved in water and the which corresponds when the hydrogel forms two phases (at temperatures equal or higher than this transition temperature LCST) [2, 4]. Due to its phase transition at said temperature, this material is of great interest for the study and development of applications in the biomedical field, since once it is in the body, this environment would provide the stimulus needed to induce the phase change in the hydrogel (average body temperature = 37.4 °C). On the other hand, hyaluronic acid (Fig. 1b), also known as hyaluronan, is a high molecular weight polysaccharide found in the extracellular matrix, especially in the soft connective tissue [7], and it is a glycosaminoglycan. It is constituted by disaccharide repeating units having the [D-glucuronic acid (1-β-3) *N*-acetyl-D-glucosamine (1-β-4)]_n structure [4, 7], and it

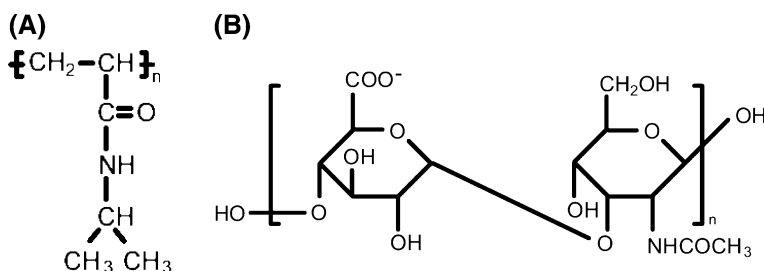


Fig. 1 Molecular structure of **a** PNIPA, **b** hyaluronic acid salt

can be obtained from different natural sources such as the vitreous humor of the eyes, the joint fluid, the rooster's comb, the umbilical cord, among others [7].

A great amount of the research on PNIPA hydrogels is focused on the hydration kinetics, because this kind of hydrogel is aimed to the controlled release of drugs, being the hydration kinetics a key element for this application [8]. However, there were found only a few research works on interpenetrating networks (IPN). In this regard, it is worth mentioning the study of Kim et al. [9] who evaluate hyaluronic acid–poly(ethylene oxide) hydrogel, showing the capabilities of these materials as biomaterials to the point of being able to create cartilage tissue.

Although nowadays there is a large amount of works on the use of PNIPA [2, 4, 5, 10–17], as well as on HA [7, 18–20], we have found few research works related to the synthesis of this polymer in the presence of the naturally occurring hyaluronic acid (HA) polymer in the reviewed literature. Ohya et al. [17] studied poly(*N*-isopropylacrylamide)-grafted hyaluronan (PNIPAM-HA) and PNIPAM-grafted gelatin (PNIPAM-gelatin), and these materials exhibit sol-to-gel transformation at physiological temperature, and they were applied as control of post-surgical tissue adhesions. Also these researchers publish about interrelationship between microscopic structure and mechanical property of surface regions and cell adhesiveness [21].

For that reason, this research work focuses on establishing what kind of biomaterial is obtained, when NIPA monomer is synthesized in the presence of HA for to obtain an interpenetrating polymer network PNIPA-HA. Study its characteristics and properties, when combining both polymers, using different well-known characterization methods, to see if it might be used as an injectable material.

Experimental procedure

Materials

The hydrogels were synthesized using ultra pure water (pH 5.6 and 17.3 M Ω /cm) as the solution medium. For the polymerization of PNIPA, *N*-isopropylacrylamide (NIPA) monomer bought from Sigma-Aldrich with a molecular weight of 113.2 g/mol was used as the starting material; ammonium peroxydisulfate (AP) as the initiator; *N,N*-tetramethylethylenediamine (TEMED) as an accelerator; and *N,N'*-methylenebisacrylamide (BIS) as the crosslinking agent in this system. The hyaluronic acid (HA) used was a purified umbilical HA purchased from Sigma-Aldrich in the form of the acid salt.

Procedure

Preparation of the hydrogels

NIPA polymerization was carried out in the presence of different concentrations of HA: 1, 2, and 3% (HA wt% based on the amount of NIPA). The different formulations are summarized in Table 1.

Table 1 Formulations prepared for synthesis of PNIPA + HA hydrogels

Material	PNIPA	PNIPA + 1%HA	PNIPA + 2%HA	PNIPA + 3%HA
Ultra pure water (ml)	17.0	17.0	17.0	17.0
NIPA (mg)	833.0	824.7	816.34	808.0
BIS (mg)	1.40	1.40	1.40	1.40
PA (mg)	6.60	6.60	6.60	6.60
TEMED (μ l)	67.0	67.0	67.0	67.0
HA (mg)	0	8.33	16.7	25.0

Formulations were chosen using the methodology proposed by Stile et al. [10] as a reference. These researchers prepared a PNIPA and PNIPA/acrylic acid hydrogel with few crosslinks to obtain a material which had the rheological properties needed to be used as an injectable hydrogel.

Formulations were synthesized in a 50-mL glass reactor under an $N_2(g)$ inert atmosphere. First, 17 mL of ultra pure water was added; then, the minority component of each formulation (HA) was added in the corresponding proportions. The system was submitted to low-speed magnetic stirring at 25 °C for about 30 min until all the HA was dissolved. Thereafter, the NIPA monomer was added to each formulation and submitted to stirring for another 40 min until it was dissolved. After the complete dissolution of these components, the crosslinking agent (BIS), then the initiator (AP) and finally the accelerator (TEMED) were added and the sample was left under stirring at an inert atmosphere reacting at room temperature for 19 h.

For to remove residual monomer NIPA (a neurotoxic monomer [6]) and any other unreacted chemicals, a dialysis process was used as sterilization step (using a Cellu-sep membrane dialysis). Thereafter, the obtained hydrogel was transferred to a container and sealed to avoid the loss of humidity.

Freeze-drying

A Labconco Freeze-Dryer 12 was used for the lyophilization process. All the hydrogel formulations were placed in sample containers, frozen and later freeze-dried for 5 days to constant weight. The hydrogels were then removed and were kept hermetically sealed in the container tubes. The weight was recorded before and after the freeze-drying, and the amount of water removed through the dehydration process was calculated.

Infrared spectroscopy (FTIR)

All the samples were analyzed with Fourier Transformed Infrared Spectroscopy (FTIR) using a Nicolet Magna-IR 750 spectrometer. In all cases, spectra were obtained collecting 32 scans with a 4 cm^{-1} resolution, and were analyzed with the help of the *Omnics* software. In order to obtain each infrared spectrum, an aliquot of the freeze-dried hydrogel (some blends contained a small portion of water) was spread on a pre-manufactured barium fluoride (Ba_2F) disk, as this material is not

affected by the remaining water. In the case of samples whose water content could not be removed completely, a part of the hydrogel was prepared to form a film, which was directly exposed to the infrared beam of the spectrometer.

Nuclear magnetic resonance (NMR)

A Bruker Avance 500 NMR spectrometer (^1H at 500.13 MHz) with a 30° pulse (3.67 μs) and a pulse delay of 1 s, 128 scans per spectrum, was used to obtain the ^1H -NMR spectra. The samples analyzed were previously freeze-dried. Once dehydrated, deuterated water (D_2O) was added to the hydrogels and they were left to hydrate and reach equilibrium, forming a very viscous solution. Essays were carried out at 25°C for all hydrogel formulations; and for the PNIPA and PNIPA + 3%AH hydrogels the spectra were obtained at four different temperatures, below and above the transition temperature (25, 30, 35, and 40°C).

Scanning electron microscopy (SEM)

Scanning electron microscopy (SEM) was used to study the porous structure of the hydrogels PNIPA and PNIPA + AH. The freeze-dried samples were cryogenically fractured in liquid N_2 , and later gold coated on Sputter-coater Balzers-SCD-030 unit, and then examined using a Phillips-S500 electron microscope, with an acceleration voltage of 20 kV.

Differential scanning calorimetry (DSC)

About 10.0 ± 0.1 mg of each formulation were weighed and placed in hermetically sealed aluminum pans. A Perkin-Elmer DSC-7 calorimeter with an ultra high purity $\text{N}_2(\text{g})$ inert environment was used. The scanning temperature range was from 20 to 50°C at a heating rate of $3^\circ\text{C}/\text{min}$, as recommended in previous studies [10, 22], to effectively verify the LCST transition. The DSC-7 was calibrated with an indium and hexatriacontane standards. Freeze-dried and rehydrated samples were used, and two samples for each formulation were analyzed for to check reproducibility.

Rheology

The rheological properties of the hydrogels were studied on a Rheometrics Dynamic Analyzer RDA-II rheometer, using plate–plate geometry with a diameter of 25 mm at 25°C . Samples were submitted to frequency sweeps (ω) in the range of 0.1–100 rad/s and at a constant strain (γ) of 20% (samples were in the linear viscoelastic range at this strain) to study the shear storage modulus (G'), the shear loss modulus (G''), the complex modulus (G^*), and the complex viscosity (η^*).

Furthermore, dynamical temperature ramp rheological tests were carried out from 25 to 50°C on a Rheometrics Dynamic Analyzer RDA-II rheometer (using the dynamic rheology temperature ramp mode) setting the following parameters: Frequency = 10.0 rad/s, initial temperature = 22.0°C , final temperature = 50.0°C , temperature ramp rate = $5.0^\circ\text{C}/\text{min}$, time per measurement = 5 s, strain = 20.0%,

transducer = Number 1. Any drying process was observing during the rheology measurements.

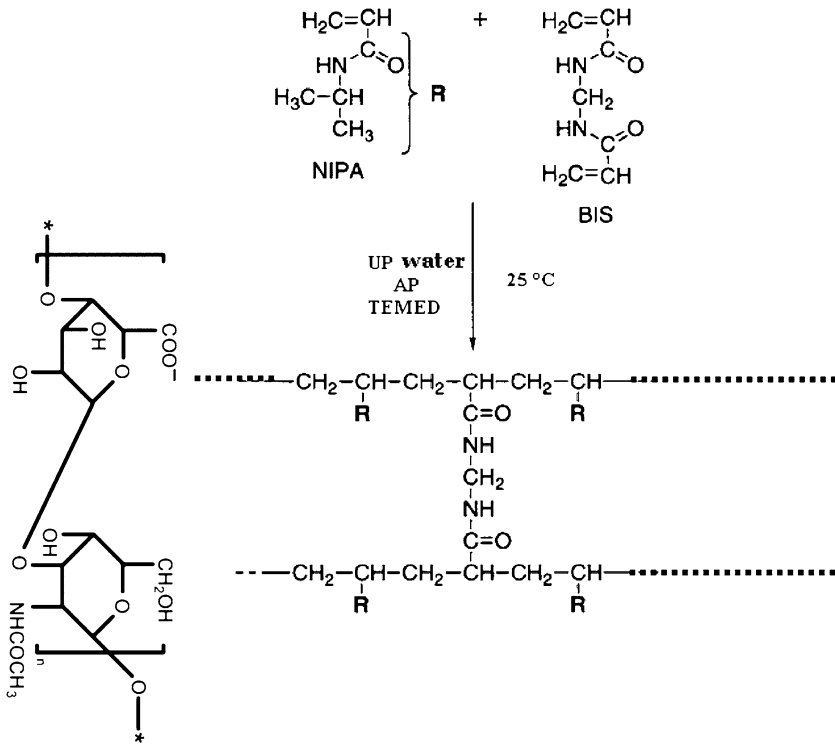
Cytotoxicity test by cell hemolysis on blood agar

Agar gel was prepared with 5% blood of healthy mice. At the same time, the hydrogels (coming from lyophilization process) were washed: they were placed in a cell culture well, 5 ml of a phosphate buffer solution 1× (PBS) was added, and the system was placed for 10 min in an oven at 37 °C (under a 5% CO₂ flow and 95% humidity). At this temperature, the hydrogel underwent a transition to a solid, which made the removal of the PBS solution easy. Once this solution was removed, the hydrogel was left to cool to room temperature, recovering its gel-like appearance (gelling and transparent). Then, the material was washed for a second and a third time with the PBS solution. Immediately thereafter, 1 mL of ethanol was added on the top of the hydrogel and the material was placed for 30 min in the laminar flow hood under UV exposure to sterilize each sample. Then, the hydrogel was washed for a fourth time with PBS (under completely aseptic conditions). Once the hydrogels were washed and sterile, they were brought into contact with a MEM culture medium and were transferred under sterile conditions to prepare the Agar blood-PNIPA gels. The blood was mixed with agar in a totally sterile medium and was gelled for 30 min, after that some grams of PNIPA and PNIPA + HA was added in the center of each gel where agar was not still solid, so the gelling was continued for another 90 min. All these processes for cytotoxic test were conducted at 37 °C using a cell culture oven (5% CO₂ flow and 95% humidity). Finally, the surface around each hydrogel sample was observed after 12, 24, and 36 h and was compared to the control (a blood agar gel which had not been in contact with any hydrogel). Results were followed as a function of time and a digital Sony camera (6.0 megapixels, 12× zoom) was used to take pictures.

Results and discussion

Synthesis

PNIPA hydrogel synthesis mechanism observed is the expected mechanism proposed by Stile et al. [10]. But in this case, the NIPA monomer could act as a macro-radical in the presence of HA (see Fig. 1), as it has active points on the chain (such as carboxylate groups, RCOO⁻) where the polymerization of the NIPA monomers may be started (or stopped) [21, 22], considerer that both NIPA and HA are highly soluble in water. Once the polymerization has started, it would propagate through a chain polymerization mechanism as was previously explained in the literature [10, 23] for the synthesis of pure NIPA. In the cases where hyaluronic acid is present, the activation of chain ends with -OH groups is expected to happen or the HA fraction may simply act as an interpenetrating phase without chemical interactions (see Scheme 1).



Scheme 1 Propose of general reaction for synthesis of PNIPAA + HA, under experimental conditions used in this study

Therefore, different PNIPAA molecular weights could be expected for different concentrations of HA, and an interpenetrating network-like structure (IPN) could be created, as the one proposed on Fig. 2.

Nuclear magnetic resonance

¹H-NMR spectra were obtained to characterize and identify the elements of the formulations.

Figure 3 corresponds to NMR spectrum of the synthesized PNIPAA used as a control. This ¹H-NMR spectrum shows peak 1 at 1.03 ppm (methyl group –CH₃ present on the isopropyl group); peak 2 at 1.47 ppm (protons –CH₂– group on the backbone); peak 3 at 1.90 ppm (proton –CH– located on the backbone); and peak 4 at 3.79 ppm (proton of the –CH– group on the isopropyl) [10, 12, 24, 25].

The integration ratio of peaks 1, 2, 3, and 4 should correspond to a 6:2:1:1 proton ratio, which defines the structure of NIPAA and confirms the structure of PNIPAA [25]. The best defined peaks correspond to impurities present in the system, since the peaks belonging to the polymers normally are wider due to the characteristics of the material [10].

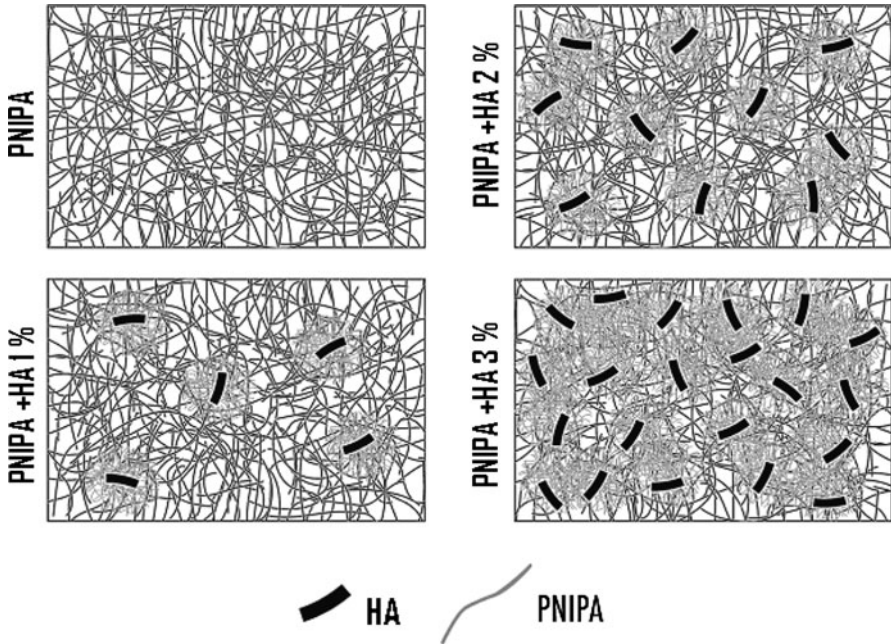


Fig. 2 Interpenetrated polymer network structure proposed for PNIPA/HA hydrogels in functions of HA concentration

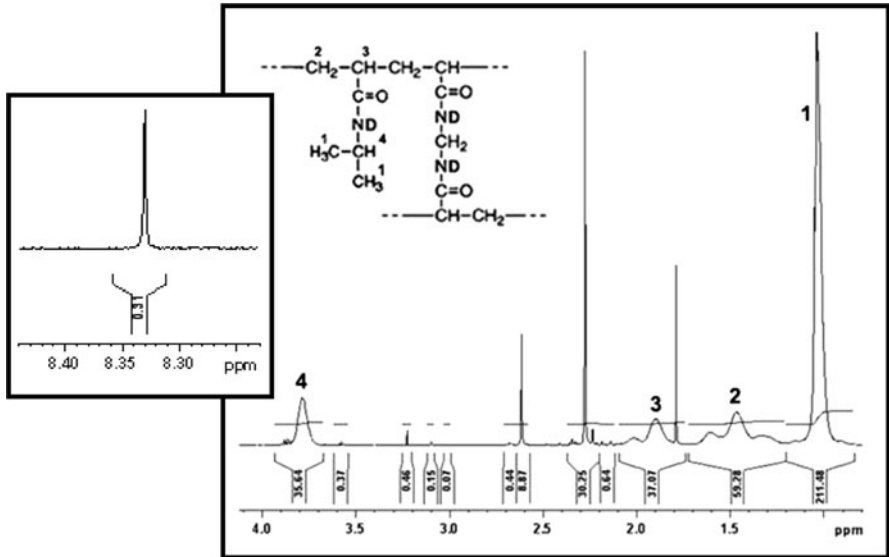


Fig. 3 ¹H-NMR spectra for synthesized poly(*N*-isopropylacrylamide)

Peaks at 2.28 and 2.61 ppm are not assigned accurately in the literature. These peaks do not appear in the spectra of the pure components; thus, they are associated to possible isomeric structures and/or chain end groups (due to the different types of possible chain ends) [8, 10, 24]. The peak corresponding to the proton of the molecule of the crosslinking agent (BIS) shows up at 4.5 ppm in the spectrum of the pure compound, and it is hidden under the peak of water in the spectrum of the PNIPA which has the same chemical shift [8].

Figure 3 (in a detail) shows the peak of NH, located at 8.22 ppm, which is assigned to the crosslinking agent BIS [8, 12, 24]. Normally, this peak does not show up, because this is one of the protons that exchanges easily with D₂O (as does the hydroxyl group, –OH). However, the fact that it only shows up on the PNIPA spectrum indicates that the PNIPA network is more rigid, and hence the diffusion of molecules toward the interior is harder. As a consequence, when this hydrogel is diluted in D₂O, the proton exchange with deuterium does not occur as easily throughout the whole structure. This is true if, and only if, the structure of the hydrogel can be rigid enough to hinder the free diffusion of the D₂O to the interior.

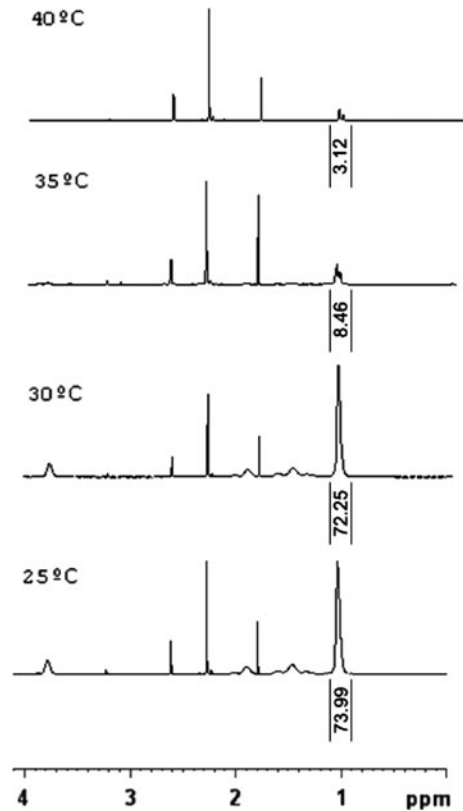
The only apparent peaks in the spectra of PNIPA + 1%AH, PNIPA + 2%AH, and PNIPA + 3%AH are those which correspond to the protons of PNIPA. This is because at these concentrations the signals which correspond to HA are not significant when compared to those of the protons in PNIPA.

¹H-NMR spectra were obtained at different temperatures (25, 30, 35, and 40 °C, ensuring that temperatures both above and below the LCST transition of PNIPA were included) to study the structural changes of the hydrogel resulting from the temperature-induced phase change (see Fig. 4). It is well known that PNIPA/water solutions show a LCST phase separation process at around 32 °C [8, 10–12]. However, the conformational change has not yet been well explained [8, 12, 24]. In this case, the phase change was evident because the solutions turned cloudy at temperatures higher than 34 °C.

There is an explanation which seems to be the most appropriate to describe the configurational changes of the PNIPA hydrogel: In a first step, the polymer chains collapse individually, and then aggregate into larger final structures constituted by aggregates [8, 12, 24]. This first stage would be characterized by the conformational transition of the polymer chains from coil to globule which was studied by Fujishige [26], who measured the radius of gyration and the “Stokes” radius of PNIPA. This researcher concluded that all the chains collapse before the system becomes thermodynamically unstable.

After this collapse and after the so-called globules are formed, they join together to create aggregates of molecules [27]. At a molecular level, when the PNIPA hydrogel exceeds the LCST temperature, a new compact structure is formed due to the displacement of the water molecules, and obstructs the internal rotation of the PNIPA chains; thus reducing the intensity of the peaks, because as the temperature rises, the material starts to behave more like a solid. Hence, the pulse ¹H-NMR technique in solution becomes less useful and, to obtain a better resolution at temperatures higher than the LCST, it is necessary to use solid state NMR. However, in this case, thanks to the pulse technique in solution it was possible to study the changes of spectra with the increase of temperature in detail.

Fig. 4 $^1\text{H-NMR}$ spectra for synthesized poly(*N*-isopropylacrylamide) hydrogel at different temperatures



The $^1\text{H-NMR}$ peaks of the PNIPA can be divided in two families: the first one, due to the functional group located at the sides of the chain as a branch (isopropyl group [8]); and the second one, due to the protons of the backbone. Both the families of peaks decrease in intensity as the temperature increases.

Figure 4 also shows that, when the temperature exceeds the LCST, all the peaks shift slightly to higher fields and become broader. This happens because the peak of water shifts slightly to higher fields (to the right) as it is very susceptible to temperature changes.

Previous studies [8, 26] have shown that the changes in the intensity of the peak (which corresponds to the proton of the methyl) are proportionally larger than those of the protons of the backbone, which implies that during the phase change the conformational changes of the isopropyl group are more significant than the conformational changes of the backbone. These studies also state that during the phase change the intensity of the peak which corresponds to the proton of water increases as the temperature rises, while the intensity of the peak which corresponds to the proton in the isopropyl group decreases with the increase of the temperature, suggesting that part of the water molecules is apparently released from the hydrated structure of the polymer chains to become part of the water solution that does not interact with the polymer. For this reason thanks to the changes in the signal of the

protons associated to the isopropyl, $^1\text{H-NMR}$ results let us observe how the water is released from the structure after the phase transition.

Figure 5 (which is a detail of Fig. 4) shows how the chemical environment of the protons of the isopropyl (~ 1 ppm) changes considerably; not only does the integral become smaller, but also the form of the peak changes; a single peak becomes two low intensity doublets. These doublets become more defined with the increase in the temperature. One of them is attributed to the isopropyl group whose movement is hindered due to the carbonyl-amide hydrogen bonds. This peak was less perceptible before and now shows a higher intensity due to the transition. The second doublet is attributed to a number of isopropyl groups, which due to their random configuration, are now no longer hindered. This shows that the isopropyl protons are in a different chemical environment when no water is around.

The same trend described earlier for the peaks of PNIPA can be seen in the PNIPA + 3%AH formulation spectra (Fig. 6), i.e., it is impossible to detect the HA peaks in any of the temperature ranges studied. It is therefore that basically the same spectra are obtained for formulations with 1%HA and 2%HA, showing exactly the same LCST transition characteristics observed around the isopropyl groups and supporting the previously provided explanation.

Fourier transformed infrared spectroscopy (FTIR)

FTIR spectra were obtained to determine the chemical structure of the hydrogels (see Figs. 7 and 8). However, not many indications were found to support the proposed explanation, mainly because, as happened with the $^1\text{H-NMR}$ spectra, the

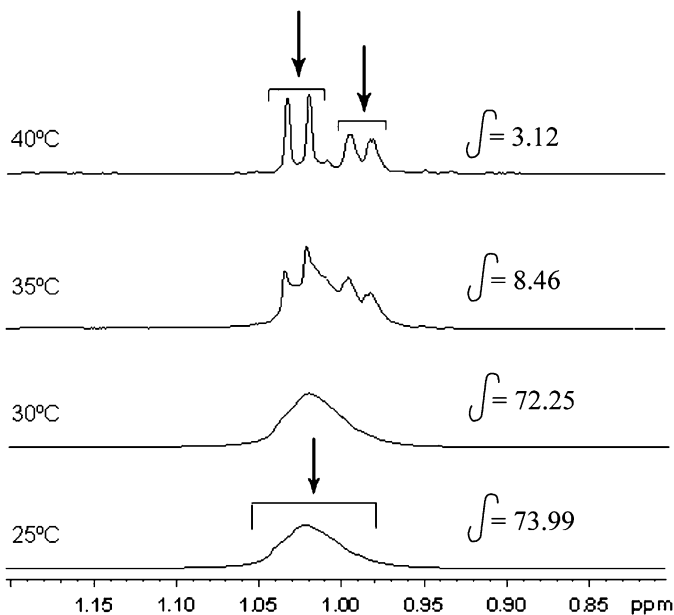


Fig. 5 Detail of $^1\text{H-NMR}$ spectra for synthesized PNIPA hydrogel at different temperatures

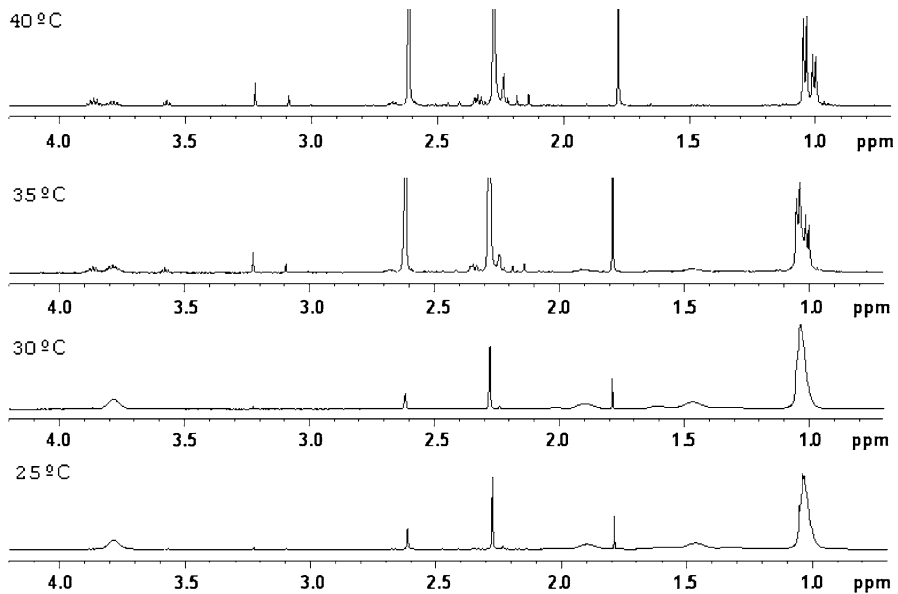


Fig. 6 $^1\text{H-NMR}$ spectra for synthesized PNIPA + 3%HA hydrogel at different temperatures. Conformational changes are observed around of the isopropyl group in function of temperature

HA percentages are so low that signals which do not correspond to PNIPA are hard to observe. Each spectrum showed the characteristic IR bands of PNIPA in agreement with the results of different published research works [12–14, 25].

In the cases in which PNIPA was reacted with HA, there appeared a characteristic signal which differentiates the spectra of these materials from PNIPA (see Fig. 8). There is the band at about 1080 cm^{-1} which corresponds to the ether

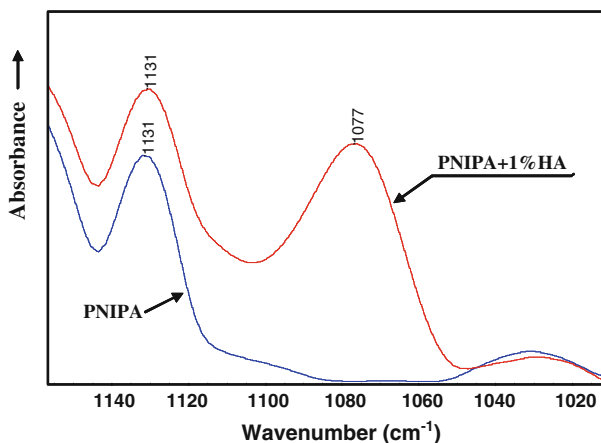


Fig. 7 FT-IR spectra around $-\text{C}-\text{O}-\text{C}-$ functional group ($\sim 1076\text{ cm}^{-1}$) for synthesized PNIPA + 1%HA hydrogel

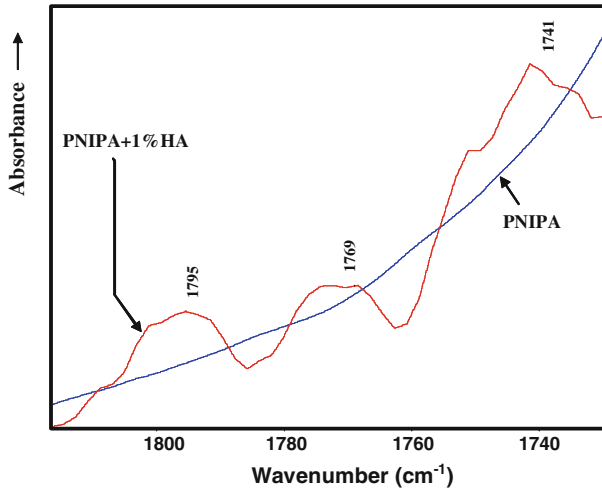


Fig. 8 FT-IR spectra around carbonyl group ($\sim 1740\text{--}1800\text{ cm}^{-1}$) for synthesized PNIP + 1% HA hydrogel

group ($-\text{C}-\text{O}-\text{C}-$), present in the chemical structure of the minority component of the hydrogels [9]. Likewise, there is also an ester group ($-\text{COOR}$) in the minority component ($\sim 1750\text{ cm}^{-1}$) as a polysaccharide [14, 28, 29] of the PNIP/HA formulation, which is not present in the PNIP.

For the synthesis of the hydrogel with HA, it has been proposed that the NIP monomers might be activated and would initiate their polymerization from active carboxylate centers (COO^-) of the HA in its acid salt form. After deconvoluting the PNIP hydrogel/HA FTIR spectrum, the presence of the $-\text{COOR}$ group (absent in the PNIP hydrogel) was detected. This signal splits into three peaks, which evidence three different chemical environments for the carbonyl of the ester group formed during the synthesis (see Fig. 8).

The three different chemical environments for the $-\text{COOR}$ group confirm that in addition to the group in its original salt form ($-\text{COO}^-$) which gives rise to a weak signal at 1597 cm^{-1} (not found in the spectrum), there are other signals arising from this group. The first signal corresponds to the interaction with the water ($-\text{COOH}$); the second signal is the one related to the groups attached to possible PNIP chains ($-\text{COOR}$); and the third signal would be related to the neighbor groups. These signals appear at about 1740 , 1769 , and 1795 cm^{-1} , respectively. The presence of these bands help to infer that the presence or formation of new vibrational modes of the $-\text{COOR}$ group is the result of the possible interaction between the carboxylate group of the HA and the growing NIP chain which is propagating from this group (explained before, and for to create a IPN network as was propose in Fig. 2). Although this evidence is necessary to infer the possible presence of covalent bonds between the PNIP and the HA, it is not enough to confirm it. It might, however, prove that the interpenetrating phase of the hydrogel, i.e., the HA molecules, interacts with the polymer network.

Water in the hydrogels

The nature of the water in the hydrogel can be determined through the permeation of fluids, nutrients, or cell products through this gel. When a dry hydrogel starts to absorb water, the first water molecules penetrating the gel matrix will hydrate the more hydrophilic and polar complexes of the system, leading to the creation of the so called primary bound water [30, 31].

After the polar groups are hydrated (primary bound water), the network starts to swell and, thanks to this swelling, the macromolecular chain disentangles and the molecules have more space to move, thus exposing the hydrophobic groups which also interact with the water molecules leading to the “bound water–hydrophobic group” interactions called “secondary bound water”. Into scientific literature it is common to encompass and simplify the terms “primary bound water” and “secondary bound water” under the terms “total bound water” or “associated water” [30].

After the polar groups have interacted with the water molecules and the hydrophobic groups are structurally forced to interact with them, another amount of water is soaked by the network due to the osmotic force which takes the chains of the gel network to infinite dilution. This additional swelling is restricted by the covalent or physical bonds, thus creating an elastic retractile force in the network and the hydrogel reaches a state of equilibrium for a specific swelling. After the gel is saturated with water which interacts with the ionic, polar, and hydrophobic groups, an additional group of molecules penetrates the gel and swells it. This water is called “free water” and it is assumed that it fills the spaces between the network chains and/or the areas of large pores, macropores, or voids [30].

It is important to remark that a hydrogel used as a matrix in tissue engineering would never dehydrate complete thanks to the highly hydrated environment that would interact with it inside of the human body, and the water composing this gel will be composed by bound water, as well as by free water.

DSC and NMR are the most used methods to measure free and bound water, although they are rather controversial [30, 32]. In this study, we used freeze-drying also and compare with DSC and NMR results. If we assume that the free water and the bound water are equally distributed throughout the gel and only the free water can be frozen (crystallized) and, therefore, released during the freeze-drying process, the frozen free water can be removed by lyophilization, and some ideas about polymerization process of NIPA in presence of HA can be extracted from this result.

Samples were weighed before and after being submitted to freeze-drying during 1 week. Figure 9 shows the percent weight change for the removed and/or free water and it clearly shows the associated water content and the free water content for PNIPA hydrogels and PNIPA hydrogels with different proportions of HA.

As PNIPA molecules are present in a higher proportion than those of HA, there is a higher amount of associated water due to the direct interactions of water with the –NH and C=O groups present in the *N*-isopropylacrylamide structure [10]. The other fundamental aspect to be considered when analyzing the effects of associated water and the results of the freeze-drying process is that the more rigid and more crosslinked a network is, the harder the movement of water will be. This, in turn, favors the interaction with the associated water, because the water is structurally

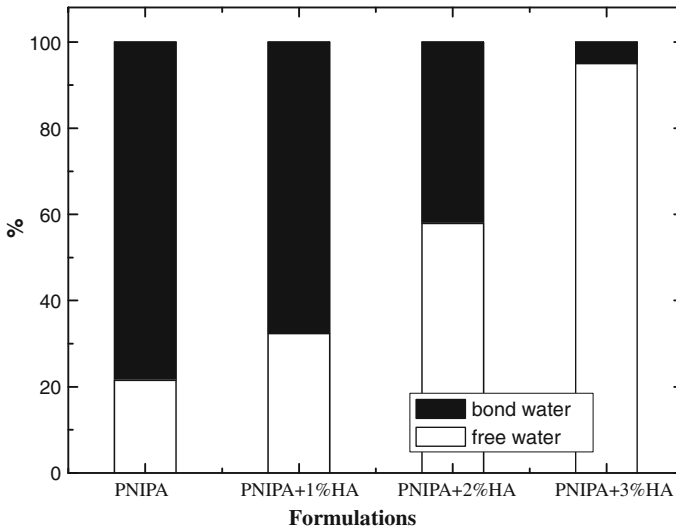


Fig. 9 Relation of associated or bond water/free water for synthesized PNIPA + HA hydrogels

being forced to stay inside the network. The initial network (PNIPA) is the most rigid and most crosslinked sample. These characteristics hinder the diffusion of water and its later removal, and this only get worse when the HA is included.

Then, it can propose that a higher amount of HA in the formulation might be interfering with the free growth of the PNIPA network during the polymerization process. As a consequence, the network looks less continuous and could have HA molecules embedded in the structural network of the PNIPA formed. This might confirm the NMR and FTIR evidences regarding the formation of an interpenetrating network IPN rather than the formation of covalent bonds between the PNIPA chain and the HA (grafting for example).

Thermal properties: differential scanning calorimetry

The solubility of PNIPA depends on the temperature [2, 3, 32]. For that cause, the study of the thermal properties of this polymer is of great interest. The transition temperature, T_t (LCST), was determined by DSC by studying the net energetic changes in the form of heat that happen during the LCST transition of the hydrogel. The transition could not be clearly identified when using a heating rate of 10 °C/min; therefore, it was reduced to 3 °C/min. This time, a transition temperature associated to a LCST type transition could be clearly seen. For the DSC results, as well as for the rheological tests which will be discussed later, the onset temperature (T_t onset) was considered to be the transition temperature, as it theoretically represents the temperature at which the LCST transition starts.

DSC thermograms showed an endotherm. This heat flow is the heat energy absorbed by the hydrogel due to the disappearance of the polymer–water interactions. This transition occurred for all the samples and appeared at an average temperature of

$T_t = 35 \pm 1$ °C which falls into the expected range similar to results obtained in previous studies [33, 34].

It is important to emphasize that it is possible to shift the transition temperature to higher or lower values by adding a new component to the PNIPA [16]. Normally, the addition of hydrophilic components to PNIPA shifts the T_t to higher temperatures, while the presence of hydrophobic components results in the opposite behavior [2]. The T_t will change depending on the nature of the secondary component to PNIPA, its proportion and the way it is incorporated into the system. It is even possible that the ability of the polymer to undergo an LCST transition might be jeopardized.

The DSC results obtained when adding different proportions of HA are shown in Fig. 10, where the transition can be clearly seen.

The endotherms show a slightly logical sequential pattern for the PNIPA, PNIPA + 1%AH, PNIPA + 2%AH, PNIPA + 3%AH formulations when the position of T_t is compared. This pattern, however, does not hold for the area under the endothermic peak (ΔH). There is only a slight difference in the position of T_t ; this slight shift may reflect the hindrance caused by the HA molecules (starting at 2%) to the mobility and the transition of the PNIPA polymer chains. As was described before, this behavior is expected: when adding a hydrophilic compound (such as the HA) to the PNIPA [35], the transition is shifted toward slightly higher temperatures. On the other hand, this slight temperature shift might be within the experimental detection error of the DSC-7 equipment (± 2 °C). These results are summarized in Table 2.

The enthalpy factor (ΔH), determines the amount of energy, in joules per grams of sample, needed for the transition. Furthermore, as the transition is related to the amount of energy necessary to break the hydrogen bonds of the associated water, it might be concluded that the higher the ΔH value, the more the associated water in

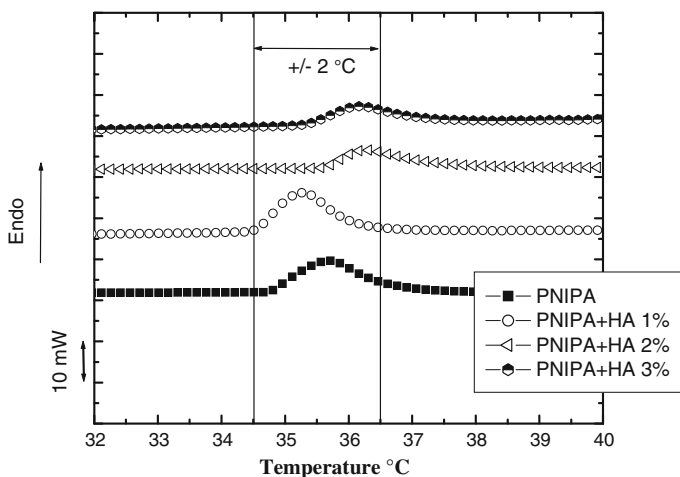


Fig. 10 DSC heating thermograms for synthesized PNIPA + HA hydrogels. LCST transition is clearly observed

Table 2 Transition temperature T_t onset extracted from DSC thermograms for synthesized PNIPA and PNIPA + HA hydrogels

Enthalpy values ΔH associated to this LCST transition

Formulations	T_t onset (°C)	ΔH (J/g) \pm 10%
PNIPA	34.7	3.0 \pm 0.3
PNIPA + 1%AH	34.4	3.0 \pm 0.3
PNIPA + 2%AH	35.5	1.4 \pm 0.14
PNIPA + 3%AH	35.3	1.0 \pm 0.1

the hydrogel. This corresponds perfectly with the results of the freeze-drying: the more HA in the formulations, the lower the amount of associated water [15, 30], as can be seen when checking the values of ΔH obtained when the HA content is $\geq 2\%$.

Additionally, it can be seen that the addition of 1, 2, and 3% of HA does not modify the general LCST transition range when compared with the PNIPA control formulation. They stay within an error range of only ± 2 °C, which suggests that the composition of hyaluronic acid into each formulation only just shifts the LCST thermal transition (T_t) of the LCST hydrogel systems when compared to the PNIPA control, but are still below the level of body temperature.

Rheological properties of PNIPA + HA hydrogels

The complex modulus G^* represents the combination of the effects of G' and G'' for a material. When the complex modulus plot is compared with the curves of G' and G'' , it is evident that it shows the same trend as G' . Thus, it could be said that for G^* the main contribution comes from the elastic component and this is the reason why G' was plotted. On the other hand, the complex viscosity reflects the stress necessary to mobilize the polymer chains as the dynamic strain rate increases in the 0.1–100 rad/s range.

As can be seen in Fig. 11, the G' curves show the same trend as the other rheological elements. PNIPA has a higher complex viscosity than the rest of the evaluated materials, which is consistent with the results shown before and is due to the fact that it has the highest degree of crosslinking and the highest molecular weights of the samples studied [36–38].

As can be seen in Fig. 12, the complex viscosity, η^* , of the studied hydrogels falls as the strain rate increases. This is because the entanglements and crosslinks break as they are submitted to a higher stress and thus the movement of the chains increases. These crosslinks and entanglements are easily lost because the interpenetrating phase of HA hinders the continuous polymerization of PNIPA, thus limiting its molecular weight and crosslinking density, as was mentioned before (and shown in the diagram in Fig. 2).

There are very few research works [17, 35] using a dynamic temperature rheological ramp to measure the LCST phase transition for PNIPA hydrogels. This method considers the chain mobility as the temperature rises and how it changes, to establish the transition temperature.

As can be seen in Fig. 13, a fast and significant change in G' (over one order of magnitude) indicates the phase transition. This evidences a sudden structural change at a temperature which lies within the reported LCST transition temperature range.

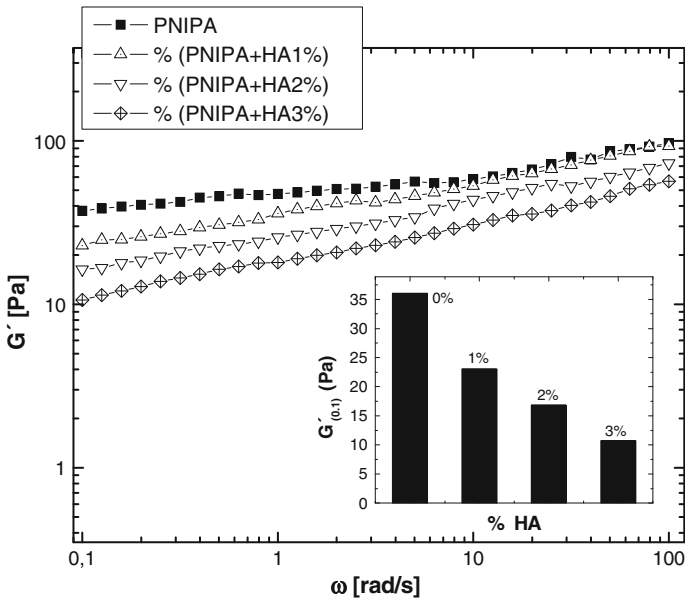


Fig. 11 Rheological behaviour (G') for synthesized PNIPA and PNIPA + HA hydrogels at $T = 25\text{ }^{\circ}\text{C}$. Inset G' values around 0.1 rad/s obtained for these hydrogels

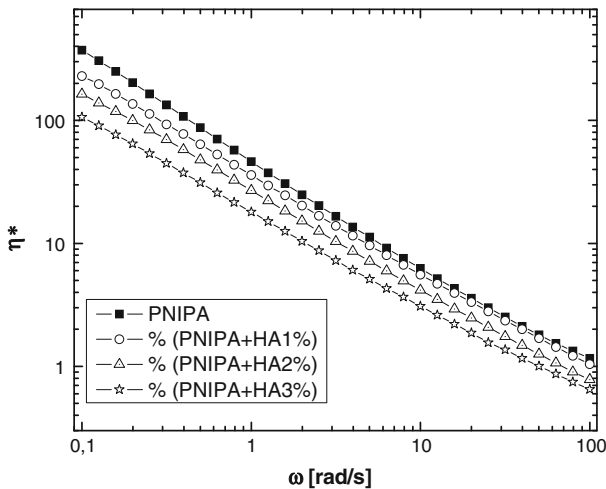
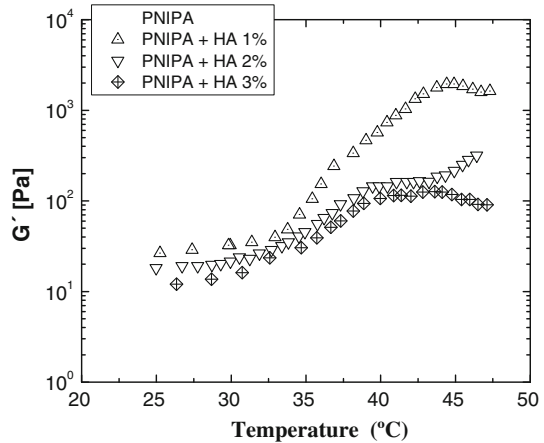


Fig. 12 Complex viscosity (η^*) behaviour for synthesized PNIPA and PNIPA + HA hydrogels at $T = 25\text{ }^{\circ}\text{C}$

As is well known, at temperatures below the T_t the PNIPA hydrogel chains are surrounded by water. This means that, when being submitted to strain, water could act as a lubricant or plasticizer between the chains, making molecular mobilization easier and thus reducing the value of G' , because the material will be behaving more

Fig. 13 Rheological behaviour (G') for synthesized PNIPA and PNIPA + HA hydrogels in function of temperatures



as a liquid than as a solid. As the temperature increases, this hydrophilic nature will change and water will be displaced. Now that water is no longer present, a higher stress is necessary to mobilize the chains, which shows as an increase in the elastic component of the modulus, G' , as the material starts to behave more like a solid.

As with DSC, and according to the rheological tests results presented, the PNIPA + 2%AH and PNIPA + 3%AH hydrogels show a T_t just a few degrees higher than the transition temperature for the neat PNIPA and the PNIPA + 1%AH. This shows that at HA concentrations $\geq 2\%$, it is a little harder for PNIPA molecules to move and the LCST phase transition needs more energy, but without loss their condition of viscous flowing material or soft hydrogel.

Morphology of the freeze-dried hydrogels by SEM

Although the conditions the hydrogels were exposed to are not exactly the same they will find in the human body, the porous morphology study by SEM is very useful to investigate their behavior. It is important to point out that this analysis is for to relate porous morphology with possible application of these materials, because all formulations shown flowing behavior in contact with water at room temperature. At body temperature (37.4 °C), PNIPA hydrogels will have a structure of a hydrogel at $T > LCST$, which is different from the structure it shows at $T < LCST$, as the temperatures at which they were observed by SEM.

The structural difference of PNIPA hydrogels at $T < LCST$ and those at $T > LCST$ by SEM has not been reported before. However, it is expected that the studied trends would keep at both temperature ranges, especially the differences observed when comparing the different hydrogel formulations. Then, it is expected that the porosity of the dehydrated hydrogel will be kept by the wet one. Structural characteristics such as the porosity, topography, and chemical nature of hydrogels are responsible for the success of their compatibility and performance as a biomaterial [17, 21]. Besides pore size, the interconnected channels in a 3D network, very important variable: if there are interconnected channels in a 3D network,

liquids could flow faster and the aqueous medium (hence nutrients) could penetrate deeper into the hydrogel [6, 21, 30].

As can be seen on the micrographs in Fig. 14, both the PNIPA and the PNIPA + HA samples are porous. However, the sample with HA shows a much higher porosity than the pure PNIPA. SEM micrographs for the samples containing 1 and 2% of HA are shown a small porosity structure is proportional to the HA content, i.e., they have morphologies in between those of PNIPA and PNIPA + 3%HA. This result lets us associate the morphology with the water loss data. At a higher porosity, water removal is easier and for this reason could show a specific orientation. Also, as is propose, less crosslink in PNIPA network could induce to create large porous, and for these reason for 2% HA a continuous porous structure is observed with oval shape that with only increasing in 1% HA this oval shape becomes an elongated shape and uniform. It can also be seen from another perspective: the higher water removal could have left a trail of larger pores, as also was observe by Fu and Soboyejo [39] a similar porous structure for PNIPA.

It is expected that the higher porosity shown by the PNIPA + 3%HA formulation will affect the biocompatibility in a positive way, because this will improve the diffusion of fluids and nutrients that will help the interaction of the hydrogel with the recipient organism [4, 22]. This adds to the fact that this is the formulation which has the most injectable behavior, as evidenced by the dynamic rheology results.

Cytotoxicity studies

Cytotoxicity tests using blood-rich agar allow verifying the degradation resulting from the actions of the cytotoxic components present in a given substance [40–43]. Hemolysins are enzymes that produce the lysis of red blood cells and they are produced after the cell decomposition. The bacteria producing these enzymes show a whitish or transparent halo due to the presence of these colonies resulting from the

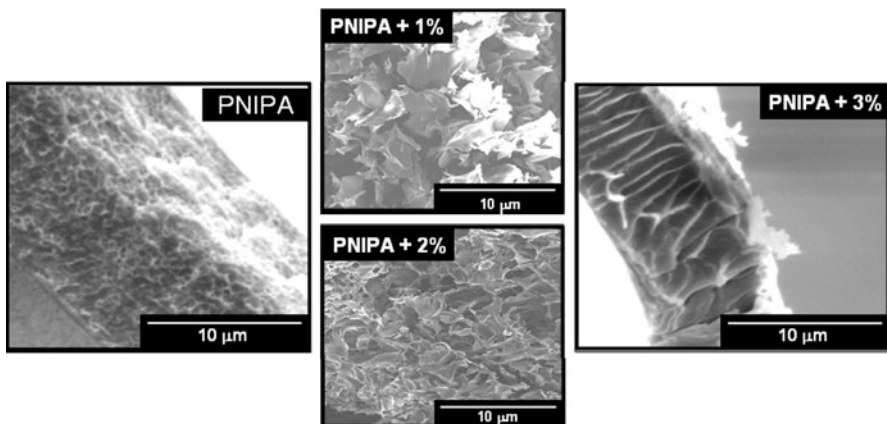
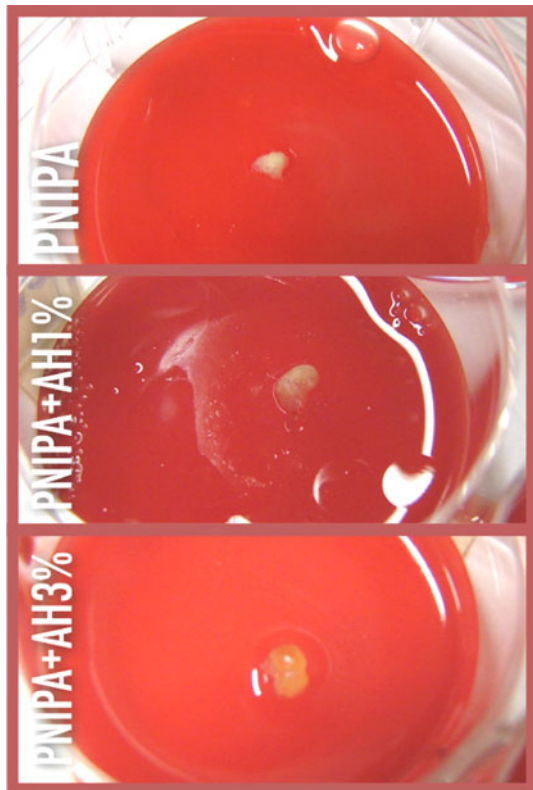


Fig. 14 SEM micrographs for dehydrated hydrogels: PNIPA and PNIPA + HA

lysis of red blood cells. Figure 15 shows the results after the hydrogels have been 36 h in contact with blood agar gel.

In this case, the possible diffusion of cytotoxic compounds from the tested hydrogels PNIP + HA would induce the lysis of red blood cells after a given time (if there is cytotoxicity), and this would be evidenced by the appearance of a whitish halo around of or close to the surface contacting the studied hydrogel. As can be seen, after 36 h in contact with the hydrogels, a whitish halo shows up around the samples containing 1% AH. This indicates that the hydrogel samples of this formulation even after a dialysis process and lyophilization, and after a series of rinses with PBS solution and MEM culture medium still release substances to the medium which are producing the lysis of the red blood cells. Therefore, when the cell membrane breaks, they leave the whitish halo or trace. In other words, the samples could still contain unreacted monomer from the synthesis of the hydrogels [17, 21, 40, 41], and for all the complex IPN network created, which makes them cytotoxic when 1% was use. But for the sample with 3% HA not showing the hemolysis effect; thus, this formulation seems to be a non-toxic, potentially injectable hydrogel.

Fig. 15 Results for cytotoxicity tests with blood-rich agar using the synthesized PNIP and PNIP + HA hydrogels, after 36 h at 37 °C and a 5% CO₂ flow in the oven for cell culture



Conclusions

We were able to synthesize smart PNIPA-based hydrogels in the presence of hyaluronic acid (HA), a natural biopolymer. The smart nature of these hydrogels is based on the LCST phase transition of these materials showed a T_t onset around 34.4–35.5 °C.

The amount of associated and of free water in the samples could be estimated through freeze-drying technique. Those hydrogels showed a clear trend, more rigid, and crosslinked structures limit water removal and, therefore, samples with these characteristics show a higher content of associated water than the structures with higher HA content, which weakens the gel network.

The functional groups of the hydrogel were identified by FTIR and $^1\text{H-NMR}$. FTIR provided non-conclusive evidence for a possible interaction of the HA with the PNIPA through the appearance of some small bands around the ester group ($-\text{COOR}$). $^1\text{H-NMR}$, DSC and a rheological temperature ramp helped to study the LCST phase transition, which remained at the same temperature even after the inclusion of the HA biopolymer.

Rheological studies also showed how the PNIPA + HA interpenetrating gels might be weakening the structure of the PNIPA hydrogel. The results allow to conclude that as the HA content increases, the elastic character represented by de storage modulus (G') and the complex viscosity (η^*) of the hydrogel decrease, thus showing characteristics of a viscoelastic system.

All results and including the cytotoxic studies show the greatest potential to be used as a non-toxic injectable hydrogel is the PNIPA + 3%HA formulation.

This research work opens an important window to the study of these hydrogels as biomaterials in the biomedical field.

Acknowledgments The authors thank Professor Alejandro J. Müller (Head of USB Polymer Group GPUSB-1, Department of Materials Science, Universidad Simón Bolívar) for providing fruitful discussions on the results here presented and for to use some equipments to characterize these samples. Also, thanks to the Decanato de Investigación y Desarrollo (DID) for their financial support through the Fund-PPI. Also thank for support from thematic IberoAmerican network BIOFAB (Biofabricação: Materiais, Processos e Simulação) funded by CYTED.

References

1. Mark H (2005) Concise encyclopedia of polymer science and technology, vol 2, 3rd edn. Wiley, New York
2. Ruel-Gariepy E, Leroux JC (2004) In situ-forming hydrogels-review of temperature-sensitive systems. *Eur J Pharm Biopharm* 58:409–426
3. Drury JL, Mooney DJ (2003) Hydrogels for tissue engineering: scaffold design variables and applications. *Biomaterials* 24:4337–4351
4. Guilherme MR, Campese GM, Radovanovic E, Rubira AF, Tambourgi EB, Muniz EC (2006) Thermo-responsive sandwiched-like membranes of IPN-PNIPAAm/PAAm hydrogels. *J Membr Sci* 275:187–194
5. Pelton R (2010) Poly(N-isopropylacrylamide) (PNIPAM) is never hydrophobic. *J Colloid Interface Sci* 348(2):673–674
6. Ratner BD, Hoffman AS (1996) Biomaterials science—an introduction to materials in medicine. Academic Press, New York

7. Manna F, Dentini M, Desideri P, De Pita O, Mortilla E, Maras B (1999) Comparative chemical evaluation of two commercially available derivatives of hyaluronic acid used for soft tissue augmentation. *J Eur Acad Dermatol Venereol* 13:183–192
8. Zeng F, Tong Z, Feng H (1997) NMR investigation of phase separation in poly(N-isopropyl acrylamide)/water solutions. *Polymer* 38:5539–5544
9. Kim WG, Choi YJ, Kim MS, Park YD, Lee KB, Kim IS, Hwang SJ, Noh I (2007) Synthesis and evaluation of hyaluronic acid–poly(ethylene oxide) hydrogel via Michael-type addition reaction. *Curr Appl Phys* 7(1):e28–e32
10. Stile RA, Burghardt WR, Healy KE (1999) Synthesis and characterization of injectable poly(N-isopropylacrylamide)-based hydrogels that support tissue formation in vitro. *Macromol* 32: 7370–7379
11. Jian H, Zhiming H, Yhongzhong B, Zhixue W (2006) Thermosensitive poly(N-isopropylacrylamide-co-acrylonitrile) hydrogels with rapid response. *Chin J Chem Eng* 4(1):87–92
12. Deshmukh MV, Vaidya AA, Kulkarni MG, Rajamohanan PR, Ganapathy S (2000) LCST in poly(N-isopropylacrylamide) copolymers: high resolution proton NMR investigations. *Polymer* 41: 7951–7960
13. Liu M, Bian F, Sheng F (2005) FTIR study on molecular structure of poly(N-isopropylacrylamide) in mixed solvent of methanol and water. *Eur Polym J* 41:283–291
14. Zareie MH, Dincer S, Piskin E (2002) Observation of phase transition of thermo-responsive poly(NIPA)–PEI block copolymers by STM. *J Colloid Interface Sci* 251:424–428
15. Suetoh Y, Shibayama M (2000) Effects of non-uniform solvation on thermal response in poly(N-isopropylacrylamide) gels. *Polymer* 41:505–510
16. Liu W, Zhang B, Lu WW, Li X, Zhu D, Yao KD, Wang Q, Zhao C, Wang C (2004) A rapid temperature-responsive sol–gel reversible poly(N-isopropyl-acrylamide)-g-methylcellulose copolymer hydrogel. *Biomaterials* 25:3005–3012
17. Ohya Sh, Sonoda H, Nakayama Y, Matsuda T (2005) The potential of poly(N-isopropylacrylamide) (PNIPAM)-grafted hyaluronan and PNIPAM-grafted gelatin in the control of post-surgical tissue adhesions. *Biomaterials* 26:655–659
18. Barbucci R, Lamponi S, Borzacchiello A, Ambrosio L, Fini M, Torricelli P, Giardino R (2002) Hyaluronic acid hydrogel in the treatment of osteoarthritis. *Biomaterials* 23:4503–4513
19. Palumbo FS, Pitarresi G, Mandracchia D, Tripodo G, Giammona C (2006) New graft copolymers of hyaluronic acid and polylactic acid: synthesis and characterization. *Carbohydr Polym* 66:379–385
20. Tan H, Ramirez CM, Miljkovic N, Li H, Rubin JP, Marra KG (2009) Thermosensitive injectable hyaluronic acid hydrogel for adipose tissue engineering. *Biomaterials* 30:6844–6845
21. Ohya Sh, Kidoaki S, Matsuda T (2005) Poly(N-isopropylacrylamide) (PNIPAM)-grafted gelatin-hydrogel surfaces: interrelationship between microscopic structure and mechanical property of surface regions and cell adhesiveness. *Biomaterials* 26:3105–3111
22. Zhang XZ, Wu DQ, Chu CC (2004) Synthesis, characterization and controlled drug release of thermosensitive IPN–PNIPA–AAm hydrogels. *Biomaterials* 25:3793–3805
23. Ní Chearúil F, Corrigan OI (2009) Thermosensitivity and release from poly N-isopropylacrylamide–polylactide copolymers. *Int J Pharm* 366(1–2):21–30
24. Starovoytova L, Spevacek J, Ilavsky M (2005) ¹H-NMR study of temperature-induced phase transitions in D₂O solutions of poly(N-isopropylmethacrylamide)/poly(N-isopropylacrylamide) mixtures and random copolymers. *Polymer* 46:677–683
25. Kesim H, Rzaev Z, Dincer S, Piskin E (2003) Functional bioengineering copolymers. II. Synthesis and characterization of amphiphilic poly(N-isopropyl acrylamide-co-maleic anhydride) and its macrobranched derivatives. *Polymer* 44:2897–2909
26. Zenga F, Tong Z, Yang X (1997) Differences in vibrational spectra of poly(N-isopropyl acrylamide) from water solution before and after phase separation. *Eur Polym J* 33(9):1553–1556
27. Winnik FM (1990) Phase transition of aqueous poly-(N-isopropylacrylamide) solutions: a study by non-radiative energy transfer. *Polymer* 31(11):2125–2134
28. Turk M, Dincer S, Yulug IG, Piskin E (2004) In vitro transfection of HeLa cells with temperature sensitive polycationic copolymers. *J Controlled Release* 96:325–340
29. Lanthong P, Nuisin R, Kiatkamjornwong S (2006) Graft copolymerization, characterization, and degradation of cassava starch-g-acrylamide/itaconic acid superabsorbents. *Carbohydr Polym* 66: 229–245
30. Hoffman AS (2002) Hydrogels for biomedical applications. *Adv Drug Deliv Rev* 54(1):3–12

31. Khalid MN, Agnely F, Yagoubi N, Grossiord JL, Couarraze G (2002) Water state characterization, swelling behavior, thermal and mechanical properties of chitosan based networks. *Eur J Pharm Sci* 15:425–432
32. Dimitrov I, Trzebicka B, Muller AHE, Dworak A, Tsvetanov CB (2007) Thermosensitive water-soluble copolymers with doubly responsive reversibly interacting entities. *Prog Polym Sci* 32: 1275–1343
33. Kara S, Pekcan O (2003) Phase transitions of *N*-isopropylacrylamide gels prepared with various crosslinker contents. *Mater Chem Phys* 80:555–559
34. Afroze F, Nies E, Berghmans H (2000) Phase transitions in the system poly(*N*-isopropylacrylamide)/ water and swelling behaviour of the corresponding networks. *J Mol Struct* 554:55–68
35. Portehault D, Petit L, Pantoustier N, Ducouret G, Lafuma F, Hourdet D (2006) Hybrid thickeners in aqueous media. *Colloids Surf A* 278:26–32
36. Aamer KA, Sardinha H, Bhatia SR, Tew GN (2004) Rheological studies of PLLA–PEO–PLLA triblock copolymer hydrogels. *Biomaterials* 25:1087–1093
37. Leone G, Delfini M, Di Cocco ME, Borioni A, Barbucci R (2008) The applicability of an amidated polysaccharide hydrogel as a cartilage substitute: structural and rheological characterization. *Carbohydr Res* 343:317–327
38. Sandolo C, Matricardi P, Alhaique F, Coviello T (2007) Dynamo-mechanical and rheological characterization of guar gum hydrogels. *Eur Polym J* 43:3355–3367
39. Fu G, Soboyejo WO (2010) Swelling and diffusion characteristics of modified poly (*N*-isopropylacrylamide) hydrogels. *Mater Sci Eng C* 30:8–13
40. Hanks CT, Watahaz JC, Suni Z (1996) In vitro models of biocompatibility: a review. *Dent Mater* 12:186–193
41. Fischer D, Li Y, Ahlemeyer B, Kriegelstein J, Kissel T (2003) In vitro cytotoxicity testing of polycations: influence of polymer structure on cell viability and hemolysis. *Biomaterials* 24:1121–1131
42. Sabino MA, Feijoo JL, Núñez O, Ajami D (2002) Interaction of fibroblast with poly(*p*-dioxanone) and its degradation products. *J Mater Sci* 37:35–40
43. Ohya S, Nakayama Y, Matsuda T (2001) Thermoresponsive artificial extracellular matrix for tissue engineering: hyaluronic acid bioconjugated with poly(*N*-isopropylacrylamide) grafts. *Biomacromolecules* 2:856–863